Journal of Cleaner Production 234 (2019) 1134–1143

Contents lists available at ScienceDirect

Journal of Cleaner Production

journal homepage: www.elsevier.com/locate/jclepro

Green scheduling model of shuttle tanker fleet considering carbon tax and variable speed factor

Xu Xin [a], Xiaoli Wang [a], Xuecheng Tian [b], Zigen Chen [c], Kang Chen [d, *]

[a] School of Economics and Management, Tongji University, Shanghai, 200092, PR China
[b] School of Economics and Management, Wuhan University, Wuhan, Hubei, 430072, PR China
[c] Transportation Engineering College, Dalian Maritime University, Dalian, Liaoning, 116026, PR China
[d] School of Shipping Economics and Management, Dalian Maritime University, Dalian, Liaoning, 116026, PR China

ARTICLE INFO

Article history:
Received 22 April 2019
Received in revised form
20 June 2019
Accepted 23 June 2019
Available online 26 June 2019

Handling Editor: Prof. Jiri Jaromir Klemeš

Keywords:
Shuttle tanker
Ship scheduling
Green scheduling
Carbon tax
Vessel speed
Column generation algorithm

ABSTRACT

Green scheduling is an important means to achieve sustainable industrial development and enhance the green efficiency of enterprises. Given the characteristics of a modern crude oil supply system, the shuttle tanker fleet green scheduling problem (FGSP) is discussed considering a carbon tax and variable tanker speed factor. To minimize the green operating cost (i.e., sum of general operating cost and carbon tax) of the tanker fleet, an integer programming model for shuttle tanker fleet green scheduling (FGSM) is established. The FGSM optimizes the number and sizes of tankers, the number and positions of floating production storage and offloading units (FPSO) at which to berth and the scheduling plan (i.e., berthing order and sailing speed) of each tanker in the fleet. Based on the column generation algorithm, a shuttle tanker fleet green scheduling algorithm is designed to solve the above model accurately. The experimental results show that considering the speed factor, the green operating cost of an example fleet decreases. For different carbon tax rates, speed optimization is an effective way to reduce the green operating cost of the fleet. The above results also show that the FGSM and algorithm can effectively solve the FGSP, improve the operation level and efficiency, and reduce the green operating cost of oil companies.

1. Introduction

The process of oil and gas extraction not only supplies energy products but also causes very large amounts of energy consumption and CO_2 emissions (Sun et al., 2018). Especially for large offshore oil fields, oil companies (decision makers) often need to use large tankers to collect oil from various oil platforms, resulting in a large amount of greenhouse gas emissions. Oil tankers accounted for approximately 13% of the nearly 1 billion tons of CO_2 emitted in 2015 (Olmer et al., 2017). At present, ships have become one of the largest sources of pollution with their high power (Deniz et al., 2010). Additionally, in response to global warming, governments around the world have introduced carbon emission control measures for vehicles in recent years (see Oreskes (2011), Zhang and Baranzini (2004), Jian et al. (2017) and Deng et al. (2015)). A carbon emission control system for greenhouse gas emissions is gradually being established with a carbon tax as the core. Motivated by this context, for decision makers, controlling the total amount of greenhouse gas emissions from transportation processes is not only related to morality and responsibility but also affects the green operating cost (i.e., the sum of the general operating cost and carbon emissions cost). Determining how to effectively control greenhouse gas emissions and improve the energy use efficiency of offshore oil production has gradually become a significant issue to academics and industry.

The intensity of greenhouse gas emissions in offshore crude oil transportation is closely related to the crude oil preliminary collection and supply system selected by a decision maker. In recent years, to pursue economies of scale and improve transportation efficiency, decision makers have often chosen the modern crude oil supply system (MOSS) with floating production storage and offloading units (FPSO, see Araújo et al. (2017) for details) as the core in large offshore oil fields. The common MOSS is mainly composed of several offshore crude oil platforms, several FPSOs, an oil tanker

* Corresponding author.
E-mail addresses: xinxu@tongji.edu.cn (X. Xin), xiaoli-wang@tongji.edu.cn (X. Wang), simontxcheng@163.com (X. Tian), cccdl2012@dlmu.edu.cn (Z. Chen), chenkang@dlmu.edu.cn (K. Chen).

https://doi.org/10.1016/j.jclepro.2019.06.275
0959-6526/

fleet and a land-based oil loading and discharging port (known as a "land-based port"). After the crude oil is mined from the platforms, it is continuously transported to the FPSOs through pipelines for preliminary processing (i.e., dehydration and sand filtration) and then temporarily stored in the cargo tanks of the FPSOs. Before the oil inventories of the cargo tanks reach their limits, the decision maker will dispatch special tankers (known as "shuttle tankers") to transport the oil back to the land-based port. Each FPSO usually has a large cargo tank (generally 5×10^4 m^3 ~2×10^5 m^3), which makes the MOSS's offshore oil storage capacity very impressive. In this situation, decision makers are allowed to invest in larger shuttle tankers in the MOSS, use more complex forms of fleet organization, and ultimately complete crude oil transfers at lower energy and green operating cost. Instead of the traditional form, crude oil collection by medium and even large shuttle tankers for continual berthing of multiple FPSOs and then transferring to the land-based port has become a new trend (see Fig. 1).

Obviously, the key to controlling the carbon emissions of the MOSS and improving the operating efficiency of the MOSS lies in the green scheduling of the shuttle tankers. In the context of considering the carbon tax factor, the decision making on this issue will face many challenges. **First, the composition of the shuttle tanker fleet is more complicated.** The collection of a carbon tax forces decision makers to carefully consider the use of large and small shuttle tankers when designing the tanker fleet. The full use of small shuttle tankers may result in high operating cost, while the full use of large tankers may increase carbon tax expenditures. Therefore, decision makers will carefully consider the proportion of large and small shuttle tankers in the fleet after considering the spatial distribution of FPSOs, the growth rate of crude oil inventories of FPSOs and the carbon tax rate. **Second, tanker sailing paths are more complicated.** In traditional systems, decision makers often aim to ensure the stability of crude oil transportation production, and they often use a "hub-and-spoke" network structure (see Fig. 1(*a*)). This structure requires the tankers to carry out small-volume and high-frequency oil transport operations between the land-based port and the platforms. The problem of no-load operation is more prominent, and the carbon emission intensity per unit of crude oil transportation is also higher. Under the consideration of the carbon tax, this operation form is obviously no longer economic. A more reasonable way should be based on large shuttle tankers, supplemented by small shuttle tankers, and using the MOSS to maximize transportation efficiency and reduce carbon emission intensity, and this approach is obviously more complex than traditional system design (see Fig. 1(*b*)). **Third, special consideration needs to be given to the speeds of the shuttle tankers (see Chang and Wang (2014)).** The tanker speed directly determines the fuel consumption, which in turn determines the carbon emissions and green operating cost of the MOSS. Researchers have demonstrated that slow steaming or speed reduction can significantly reduce fuel consumption and result in emissions reduction (Corbett et al., 2009). As governments impose a carbon tax, the weight of the speed adjustment on the operating cost of the MOSS further increases. If the tanker speed can be set reasonably, the shuttle tanker fleet can achieve an ideal balance between cost and scale, thereby minimizing greenhouse gas emissions and improving the operational efficiency of the MOSS. Therefore, designing a reasonable speed plan for each tanker according to actual needs becomes another problem that cannot be ignored for decision makers.

We conduct research on the above three challenges to discuss the shuttle tanker fleet green scheduling problem (FGSP) considering complex network structures and speed setting factors in the context of carbon tax collection. Specifically, under the condition of considering FPSO inventory constraints, the minimum green operating cost of the MOSS is taken as the goal, and the number of tankers, the type of each tanker, the order of berthing of FPSOs for each tanker and the speed selection of each tanker during navigation are determined. The major contributions of this paper are as follows:

- A mathematical model is established to optimize the scheduling of a shuttle tanker fleet taking the carbon tax and vessel speed factors into account.
- Using the column generation algorithm (CGA) framework, an algorithm is designed that can accurately solve the model.

In the remainder of this paper, Section 2 reviews the related literature. Section 3 conducts a detailed analysis of the MOSS, introduces a discrete method of variables to simplify the problem, and gives a mathematical expression of partial constraints. Section 4 establishes a mathematical model of the FGSP. The algorithm for solving the mathematical model is introduced in Section 5. In Section 6, a case analysis is carried out to test the applicability and effectiveness of the model and the algorithm. Finally, Section 7 concludes the paper.

2. Literature review

For the control of CO_2 emissions, some scholars have adopted

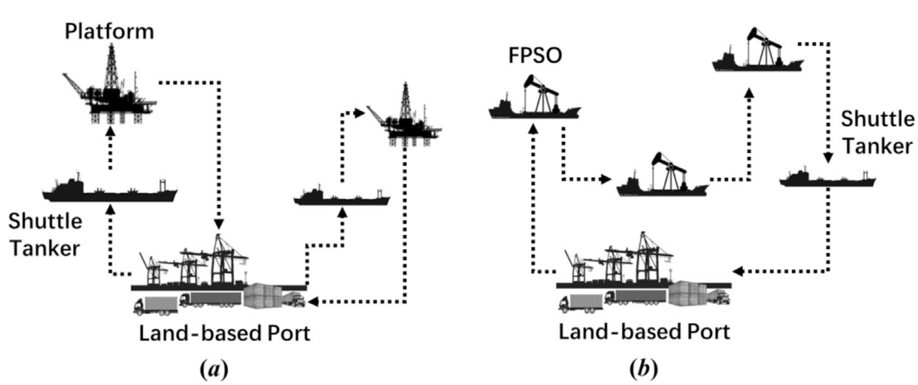

Fig. 1. Schematic diagram of the tanker fleet operation mode in a traditional system (*a*) and the MOSS (*b*).

the green method of CO_2 removal (see Sepehri and Sarrafzadeh (2018)). However, we will start from the management theory and explore FGSP from the perspective of optimizing transportation resources. We regard FGSP as an extension of a maritime inventory routing problem (MIRP). According to the definition given by Christiansen et al. (2013), an MIRP is defined as a planning problem in which an actor takes responsibility for both the inventory management at one or both ends of the maritime transportation legs and for the ships' routing and scheduling. Early research on MIRPs can be found in Christiansen et al. (2004), Ronen (1983), and Hoff et al. (2010). In recent years, research on MIRPs is still very active. For example, Alvarez et al. (2011) proposed a mixed integer model of a multiperiod fleet sizing and deployment problem, but the author did not consider the ships' routing problem. Tirado et al. (2013) developed a dynamic and stochastic maritime transportation problem and introduced three heuristics for this problem to minimize transportation cost. Given the average speed of a fleet and that of a ship, the model was able to optimize the running path of each ship under the time window of the loading and unloading at each port. Recently, Zhang et al. (2018) studied an MIRP that considered a delivery time window constraint and tried to optimize the scheduling plan of each ship. Unlike previous studies, the authors considered the factor of unpredictable disruptions. However, most of the above studies regarded the speed factor as a constant and did not take environmental factors into consideration.

In response to the above shortcomings, Bektaş and Laporte (2011) proposed a vehicle routing problem (VRP) that considered a pollution factor and called this problem the pollution-routing problem (PRP). In the PRP, the authors regarded the driving speed of a vehicle as the decision variable and introduced vehicle speed and pollutant emission functions to characterize the degree of contamination of the environment by changes in vehicle speed. This model can be used to analyze MIRPs considering a speed factor. Similarly, Fagerholt et al. (2010) proposed a speed optimization model considering a carbon emission factor for a shipping system. Given a shipping route consisting of a sequence of ports with a time window, the model could give the optimal speed for each waterway link. Brouer et al. (2013) gave a more complete solution. They discretized the ship's optional speed and then introduced the "speed link" when constructing the network model. In other words, if a ship has two optional speeds, two links would be introduced from port i to j, and different sailing times are set for each link to characterize the decision maker's choice of speed. Unfortunately, the approach proposed by Brouer et al. (2013) was designed for liner shipping systems and did not take into account changes in transportation demand and the impact of inventory factors on speed optimization.

In summary, existing research has intensively studied MIRPs from different angles, and many important and feasible solutions have been proposed. However, these solutions are not suitable for solving the FGSP. The reason is mainly because in the FGSP, the crude oil inventory of the FPSO has a strict upper bound. If the crude oil inventory reaches the upper limit, the relevant crude oil platform will be forced to temporarily stop production. Therefore, decision makers need to accurately coordinate fleet designs and tanker travel routes while satisfying the FPSO inventory constraints. Additionally, tanker speed selection and adjustment must be considered when formulating a scheduling plan.

3. Problem description

For the convenience of readers, the notations frequently used in this paper are listed as follows.

Sets	
I	Set of transport nodes
I^-	Set of FPSOs
K	Set of shuttle tankers
S	Set of alternative speeds
V	Set of alternative voyages
Parameters and Variables	
x_{ijks}	A $(0-1)$ variable, which is taken as 1 when the voyage k contains a waterway link from the transport nodes i to j and the speed is set to s.
z_{kv}	A $(0-1)$ variable, which is taken as 1 when the voyage k is executed by the tanker v.
t_i^T	The time when the i^{th} FPSO is berthed
t_{ik}^c	The time when node i is first berthed in voyage k
t_i^f	The time of the crude oil extraction operation required for the tanker when berthed at node i
t_{ijs}	The sailing time from nodes i to j when the speed is set to s
q_v	The capacity of tanker v

We split the MOSS into two subsystems. The first is a crude oil storage subsystem centered on FPSOs. In this subsystem, the main constraint that decision makers need to consider is the inventory upper bound of each FPSO's cargo tank. The second is a crude oil collection and distribution subsystem centered on the shuttle tanker fleet. In this subsystem, the important decision variable is the fleet scheduling plan. The main constraints to be considered are the time when a tanker carries out the transportation plan and the tanker's capacity. The shuttle tanker fleet consists of several tankers of varying sizes and variable speeds. After a given transportation system's operational cycle (known as a "planning period"), a tanker will carry out the transportation plan in accordance with the preset scheduling plan. The scheduling plan specifies in detail when, at what speed, and in what order each FPSO is berthed by tankers. As shown in Fig. 2, if the MOSS is abstractly viewed as a transport system in a VRP that considers inventory factors, then the crude storage subsystem can be viewed as a system including "supply points" (FPSOs) and a "central warehouse" (land-based port). Each "supply point" generates transportation demand (crude oil) at a fixed rate that is temporarily stored in the "warehouse" (FPSO's cargo tank) of the "supply point" for transport.

Let $G^R = \{I, E\}$ represent the transport network of the MOSS, where $I = \{0\} \cup I^-$ is the set of transport nodes and its elements are recorded as i or j. $\{0\}$ is the set of the land-based port, and I^- is the set of FPSOs. E represents the set of waterway links. During the planning period, the inventory change in the cargo tank of the i^{th} FPSO can be characterized by introducing a time window constraint. In other words, the constraints in **Constraint Group 1**

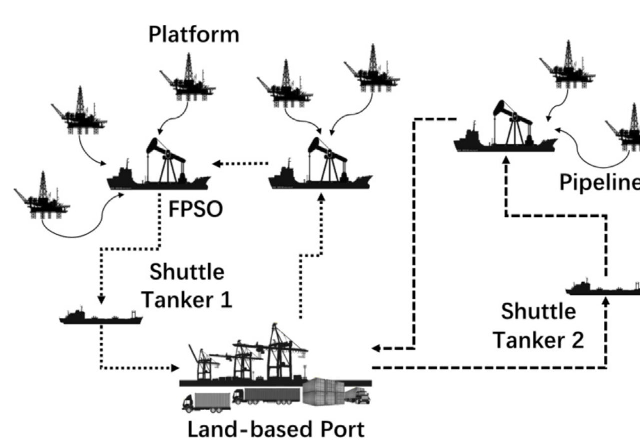

Fig. 2. Schematic diagram of the MOSS.

need to be satisfied. Here, t_i^T represents the time when the i^{th} FPSO is berthed. lb_i and ub_i represent the lower and upper bounds of the time at which the i^{th} FPSO is allowed to berth, that is, the time at which the FPSO begins to stock up (due to the continued growth of inventory, usually lb_i is 0) and the full load time, respectively. Constraints formula (1) and formula (2) are used to control the effect that each FPSO must not be fully loaded.

Constraint Group 1: constraints in the crude oil storage subsystem

$$t_i^T \geq lb_i \ \forall i \in I^- \tag{1}$$

$$t_i^T \leq ub_i \ \forall i \in I^- \tag{2}$$

The crude oil collection and distribution subsystem consists of a shuttle tanker fleet, which operates in a similar manner to the transport process of trucks in a VRP. The subsystem arranges the tankers for berthing with the FPSOs for crude oil transportation according to the established fleet scheduling plan. We assume that the speed of each tanker on a waterway link is composed of several optional speeds s and that the speed of a tanker on a waterway link is constant. The set consisting of all s is denoted as S. To characterize a ship's sailing paths, based on G^R and S, we introduce the concept of *voyage*. This concept refers to the scheduling plan of a tanker on several waterway links according to the established speed parameters, and the start and end points of a voyage must be the land-based port.

Let v denote the shuttle tanker, V denote the set consisting of all alternative shuttle tankers, and K denote the set of all voyages that can be formed in G^R. The set of all voyages executed by the tanker v during the planning period is called the single-ship scheduling plan of the tanker v, and this plan is denoted as G_v; apparently, $G_v \subseteq K$. Similarly, the set of single-ship scheduling plans for each tanker during the planning period is called the fleet scheduling plan, which is recorded as G_V^T; then, $G_v \subseteq G_V^T \subseteq K$. For any element in K, the constraints in **Constraint Group 2** must be satisfied. According to constraints formula (1) and formula (2), if $ub_i \leq T$, then the i^{th} FPSO must be berthed during the planning period, and we use B_C to represent the set of these FPSOs. x_{ijks} is a $(0-1)$ variable, which is taken as 1 when the voyage k contains a waterway link from the transport nodes i to j and the speed is set to s; otherwise, this variable is taken as 0. Here, constraints formula (3) and formula (4) require that any voyage must satisfy this definition. Constraint formula (5) ensures continuity of the waterway links during navigation. Constraint formula (6) ensures that each FPSO is berthed only once during the planning period. Here, we assume that the FPSO's crude oil inventory level is much smaller than the ship's carrying capacity. Constraint formula (7) requires that the FPSO in B_C must be berthed during the planning period to ensure continuous production of the crude oil storage subsystem. Constraint formula (8) is a $(0-1)$ constraint.

Constraint Group 2: constraints that ensure voyages are feasible

$$\sum_{j \in I^-} \sum_{s \in S} x_{0jks} = 1 \ \forall k \in K \tag{3}$$

$$\sum_{i \in I^-} \sum_{s \in S} x_{i0ks} = 1 \ \forall k \in K \tag{4}$$

$$\sum_{i \in I^-} \sum_{s \in S} x_{ijks} = \sum_{i \in I^-} \sum_{s \in S} x_{jiks} \ \forall j \in I, k \in K \tag{5}$$

$$\sum_{j \in I} \sum_{k \in K} \sum_{s \in S} x_{ijks} \leq 1 \ \forall i \in I^- \tag{6}$$

$$\sum_{j \in I} \sum_{k \in K} \sum_{s \in S} x_{ijks} = 1 \ \forall i \in B_C \tag{7}$$

$$x_{ijks} \in \{0,1\} \forall i,j \in I, k \in K, s \in S \tag{8}$$

Constraint Group 2 determines the total feasible voyage k but does not establish the connection between the voyages and the shuttle tankers. In **Constraint Group 3**, the voyages in K and the shuttle tankers are matched. We introduce a $(0-1)$ variable z_{kv}. If the voyage k is executed by the shuttle tanker v, then z_{kv} is 1; otherwise, it is 0. Constraint formula (9) requires that each voyage be executed by only one tanker. Constraint formula (10) is a $(0-1)$ constraint.

Constraint Group 3: constraints to ensure that the voyages match the shuttle tankers

$$\sum_{v \in V} z_{kv} \leq 1 \ \forall k \in K \tag{9}$$

$$z_{kv} \in \{0,1\} \ \forall k \in K, v \in V \tag{10}$$

Based on the above settings, tanker v may perform several voyages during the planning period. To ensure that each voyage arranged for each tanker can be carried out (no time conflict occurs), the critical time nodes of each voyage must satisfy the constraints in **Constraint Group 4**. Let i and j represent the numbers of the transport nodes. t_{ik}^c represents the moment when node i is first berthed in voyage k. t_i^f represents the time of the crude oil extraction operation required for the tanker when berthed at node i. In particular, no crude oil is required to be extracted at the land-based port, so $t_0^f = 0$. t_{ijs} represents the sum of the navigation time required for the tanker to sail from node i to node j at speed s and the berth time at node j. M represents a large positive number. We assume that the oil unloading time of the tanker in the land-based port is linear with the amount of crude oil, and t_k^u is used to indicate the unloading time required at the land-based port when the shuttle tanker executes voyage k. R_i^u represents the oil production of node i per unit time. b_i represents the oil storage of node i at the beginning of the planning period. t^u represents the time required to unload a unit of crude oil at the land-based port. q_v represents the capacity of tanker v. Constraint formula (11) ensures continuity of navigation time in a voyage. Constraint formula (12) requires that the same tanker does not conflict when sailing on different voyages during the planning period. Constraint formula (13) is used to calculate the unloading time of voyage k at the land-based port. Constraint formula (14) requires that the end of each voyage must not exceed the planning period. Constraint formula (15) is used to indicate that the amount of crude oil loaded by the tanker during each voyage cannot exceed its capacity. Here, we assume that the crude oil in an FPSO is completely evacuated when a tanker berths with the FPSO. It should be noted that in practice, the unloading speed of a tanker berthing with an FPSO can reach several thousand tons per hour or even more than 10,000 tons per hour, and the berthing operation time of a single tanker at an FPSO platform is short. To simplify the problem, we do not consider the situation where a tanker is waiting in line at an FPSO to unload oil.

Constraint Group 4: constraints of tanker berthing time

$$t_{ik}^{c}+t_{i}^{f}+t_{ijs}\le t_{jk}^{c}+M\left(1-x_{ijks}\right)\ \forall i\in I,j\in I^{-},k\in K,s\in S \tag{11}$$

$$t_{ik}^{c}+t_{i}^{f}+t_{i0s}+t_{k}^{u}\le t_{0k'}^{c}+M(3-x_{i0ks}-z_{kv}-z_{k'v})\ \forall i\in I^{-},k<k'\in K,s\in S,v\in V \tag{12}$$

$$t_{k}^{u}=\sum_{i\in I^{-}}\sum_{j\in I^{-}}\sum_{s\in S}\left(t_{ik}^{c}R_{i}^{u}+x_{ijks}b_{i}\right)\Big/t^{u}\ \forall k\in K \tag{13}$$

$$t_{ik}^{c}+t_{i}^{f}+t_{i0s}\le T+M(1-x_{i0ks})\ \forall i\in I^{-},k\in K,s\in S \tag{14}$$

$$\sum_{i\in I^{-}}\sum_{j\in I^{-}}\sum_{s\in S}\left(t_{ik}^{c}R_{i}^{u}+x_{ijks}b_{i}\right)\le\sum_{v\in V}q_{v}z_{kv}\forall k\in K \tag{15}$$

At this point, the decision variables t_{ik}^{c} and t_{i}^{T} related to the berthing time are introduced. However, when an FPSO is not berthed during the planning period or is not berthed in voyage k, the values of the above variables are meaningless. To deal with the above situation, we use **Constraint Group 5** to control these values. Constraints formula (16) and formula (17) together constitute a constraint on the value of t_{ik}^{c}. When voyage k does not berth the i^{th} FPSO, let $t_{ik}^{c}=0$. Constraints formula (18) to formula (21) are used to describe the relationship between t_{i}^{T} and t_{ik}^{c}. When voyage k berths the i^{th} FPSO, constraints formula (18) and formula (19) make $t_{i}^{T}=t_{ik}^{c}$; otherwise, constraints formula (20) and formula (21) make $t_{i}^{T}=0$.

Constraint Group 5: constraints on the relationship between $\mathbf{t_{ik}^{c}}$ and $\mathbf{t_{i}^{T}}$

$$t_{ik}^{c}\le M\sum_{j\in I}\sum_{s\in S}x_{ijks}\ \forall i\in I^{-},k\in K \tag{16}$$

$$t_{ik}^{c}\ge 0\ \forall i\in I^{-},k\in K \tag{17}$$

$$t_{i}^{T}\le t_{ik}^{c}\ \forall i\in I^{-},k\in K \tag{18}$$

$$t_{i}^{T}\ge t_{ik}^{c}-M\left(1-\sum_{j\in I}\sum_{s\in S}x_{ijks}\right)\ \forall i\in I^{-},k\in K \tag{19}$$

$$t_{i}^{T}\ge 0\ \forall i\in I^{-} \tag{20}$$

$$t_{i}^{T}\le M\sum_{j\in I}\sum_{s\in S}x_{ijks}\ \forall i\in I^{-},k\in K \tag{21}$$

Based on the above constraints and definitions, we can give a mathematical description of the FGSP. Under the premise that V, S, I, T and other information are known and that the MOSS does not stop production during the planning period, G_{V}^{T} is optimized and the lowest green operating cost of the MOSS in planning period T can be achieved. In other words, the FGSP aims to minimize the green operating cost of the MOSS during the planning period and to determine the shuttle tanker fleet scheduling plan G_{V}^{T} based on the transportation time window of each FPSO.

4. Model establishment

4.1. Assumptions

Based on the above discussion, we establish a shuttle tanker fleet green scheduling model (FGSM). In addition to the assumptions introduced earlier, the FGSM also uses the following assumptions:

I. The amount of crude oil in each FPSO increases linearly with time during loading.
II. The oil unloading time of a tanker in port is linear with the amount of oil discharged.
III. The tanker berthing time is included in the sailing time.
IV. The situation where a tanker is waiting in line at the land-based port or an FPSO for unloading operations is excluded.
V. The decision maker has a variety of models and enough tankers to form a fleet.

4.2. FGSM

$$\min:\sum_{i\in I,j\in I,k\in K,s\in S,v\in V}\left(c_{vs}^{F}+c_{vs}^{V}\right)t_{ijs}x_{ijks}z_{kv} \tag{22}$$

where t_{ijs} is the sailing time from nodes i to j and the speed is set to s.

Formula (22) is the objective function and aims to minimize the total green operating cost of the MOSS during the planning period. The green operating cost of the shuttle tanker consists of the fixed cost c_{vs}^{F} (mainly the operating cost) per unit time and the variable cost c_{vs}^{V} (mainly the fuel cost and carbon tax) per unit time when tanker v travels at speed s. These costs are closely related to the ship type selection and speed setting of the shuttle tanker. Since formula (22) contains decision variables x_{ijks} and z_{kv}, to linearize the objective function, we change these variables to a $(0-1)$ variable w_{ijk}^{sv}, where $w_{ijk}^{sv}=x_{ijks}\cdot z_{kv}$; then, the form of the objective function is as shown in formula (23).

$$\min:\sum_{i\in I,j\in I,k\in K,s\in S,v\in V}\left(c_{vs}^{F}+c_{vs}^{V}\right)t_{ijs}w_{ijk}^{sv} \tag{23}$$

The constraints of the FGSM include **Constraint Group 6**, which comprises constraints that linearize objective function formula (22), in addition to the constraints given above. The converted FGSM is a linear integer programming model.

Constraint Group 6: linearization constraints of the objective function

$$w_{ijk}^{sv}\ge 1/2\left(x_{ijks}+z_{kv}\right)-1/2\ \forall i,j\in I,k\in K,s\in S,v\in V \tag{24}$$

$$w_{ijk}^{sv}\le 1/2\left(x_{ijks}+z_{kv}\right)\ \forall i,j\in I,k\in K,s\in S,v\in V \tag{25}$$

$$w_{ijk}^{sv}\in\{0,1\}\forall i,j\in I,k\in K,s\in S,v\in V \tag{26}$$

5. Algorithm design

5.1. Basic concepts and algorithm flows

The FGSM is a large-scale linear integer programming model (a knapsack problem model) that cannot be solved directly using a commercial solver (e.g., Gurobi). One of the common ideas for such a complex model is to design a heuristic algorithm (such as a genetic algorithm and tabu search algorithm, see Niu et al. (2018), Li et al. (2018) and Xiao and Konak (2017)). However, these algorithms cannot theoretically guarantee an optimal solution. In 1958, Ford and Fulkerson first proposed the use of the CGA (see Ford and Fulkerson (1958)) in a multicommodity network flow problem in *Management Science*. After decades of development, the CGA has become the mainstream method used in vehicle routing design, staff scheduling, and other linear integer programming problems. Since this method can find an optimal solution, we design an FGSA that can accurately solve the FGSM based on the framework of the CGA.

The core idea of the CGA is as follows: First, the linear integer programming is split into two models — the restricted main model (RMM) and the submodel (SM) (see Agarwal and Ergun (2008) for details). Second, the dual variable value (shadow price) is obtained by solving the RMM and is substituted into the SM. Third, the result obtained by the SM is continuously added to the RMM by adding a "column" (coefficient matrix). After repeated iterations between the two models, the optimal solution of the original problem can be obtained. The basic framework of the FGSA designed in this paper is similar to that of the classic CGA. By continuously solving the SM, the FGSA obtains new single-ship scheduling plans and adds them to the RMM, and this process eventually leads to the optimal shuttle tanker fleet scheduling plan G_V^T. The basic process of the FGSA is as follows:

Step 0: Initialization. Create a feasible single-ship scheduling plan $\widehat{G}_v^0$ at random, and create a set $P = \left\{\widehat{G}_v^0\right\}$.

Step 1: Solve the FGSM-RMM. Based on P, the FGSM-RMM of column generation is solved, and the shadow price of each constraint in the FGSM-RMM is obtained.

Step 2: Solve the FGSM-SM. Based on the shadow price calculated in **Step 1**, solve the FGSM-SM and obtain a new single-ship scheduling plan $\widehat{G}_v^i$.

Step 3: Observe the objective function value of the FGSM-SM. If the objective function value of the FGSM-SM is negative, execute **Step 3.1**; otherwise, execute **Step 3.2**.

Step 3.1: Add $\widehat{G}_v^i$ into P, and return to **Step 1**.

Step 3.2: The solution of the FGSM-RMM is the optimal solution, and the FGSA is stopped.

5.2. Establish the restricted main model and submodel

In the FGSM-RMM, the set of currently known feasible single-ship scheduling plans is denoted P, and an element is denoted$p$. The decision variable y_p is a $(0-1)$ variable. If p is executed in the optimal tanker-fleet scheduling plan, then y_p is 1; otherwise, it is 0.

$$a_{ip} = \begin{cases} 1, & \text{Single} - \text{ship scheduling plan } p \text{ require a shuttle tanker berthing with the } i^{th} \text{ FPSO} \\ 0, & \text{Otherwise} \end{cases}$$

Since P is known, we also introduce the following variables and treat them as known, with the remaining symbols being the same as before:

$$r_{pv} = \begin{cases} 1, & \text{Single} - \text{ship operation plan } p \text{ use shuttle tanker } v \\ 0, & \text{Otherwise} \end{cases}$$

t_p^s: time of sailing at speed s in single-ship scheduling plan p

The mathematical expression of the restricted master model (FGSM-RMM) is as shown in below:

[FGSM-RMM]:

$$min: \sum_{p\in P}\sum_{v\in V}\sum_{s\in S}\left(c_{vs}^F + c_{vs}^V\right)t_p^s r_{pv} y_p \tag{27}$$

$$s.t. \sum_{p\in P} a_{ip} y_p \geq 1 \ \forall i\in B_C \tag{28}$$

$$\sum_{p\in P} r_{pv} y_p \leq 1 \ \forall v\in V \tag{29}$$

$$y_p\in\{0,1\} \tag{30}$$

In the above formulas, formula (27) is the objective function. Its goal is the same as the objective of formula (23), and it is required to minimize the green operating cost of the shuttle tanker fleet during the planning period. Its form is similar to that of the FGSM, except that K is replaced with P. Constraint formula (28) ensures that the FPSOs in B_C must be berthed during the planning period. Constraint formula (29) ensures that each shuttle tanker can only perform one single-ship scheduling plan. Constraint formula (30) is a $(0-1)$ constraint. The FGSM-RMM is a linear integer programming model. Due to the limited size of the problem, this model can be solved directly by a commercial solver (e.g., Gurobi).

The mathematical expression of the FGSM-SM is as shown below. For completeness and convenience, we repeat some previously presented constraints here. In the FGSM-SM, the following variables are introduced, and the remaining symbols are as previously given:

$\tilde{p}$: the new single-ship scheduling plan (new "column") that the FGSM-SM intends to generate

$\pi_i^{(28)}$: the shadow price obtained by solving constraint formula (28)

$\pi_v^{(29)}$ the shadow price obtained by solving constraint formula (29)[FGSM-SM]:

$$min: \sum_{i\in I, j\in I, s\in S, v\in V}\left(c^F_{vs}+c^V_{vs}\right)t_{ijs}x_{ijp^\sim s}r_{p^\sim v}-\sum_{i\in B_C}\pi_i^{(28)}a_{ip^\sim}-\sum_{v\in V}\pi_v^{(29)}r_{p^\sim v} \quad (31)$$

$$s.t.\ t_i^T\ge lb_i\ \forall i\in I^- \quad (32)$$

$$t_i^T\le ub_i\ \forall i\in I^- \quad (33)$$

$$\sum_{v\in V}r_{\tilde{p}v}=1 \quad (34)$$

$$r_{\tilde{p}v}\in\{0,1\}\ \forall v\in V \quad (35)$$

$$\sum_{j\in I^-}\sum_{s\in S}x_{0j\tilde{p}s}=1 \quad (36)$$

$$\sum_{i\in I^-}\sum_{s\in S}x_{i0\tilde{p}s}=1 \quad (37)$$

$$\sum_{j\in I^-}\sum_{s\in S}x_{ij\tilde{p}s}=\sum_{j\in I^-}\sum_{s\in S}x_{ji\tilde{p}s}\ \forall i\in I \quad (38)$$

$$a_{i\tilde{p}}=\sum_{j\in I}\sum_{s\in S}x_{ij\tilde{p}s}\ \forall i\in I^- \quad (39)$$

$$a_{i\tilde{p}}\in\{0,1\}\ \forall i\in I^- \quad (40)$$

$$x_{ij\tilde{p}s}\in\{0,1\}\ \forall i,j\in I,s\in S \quad (41)$$

$$t^c_{i\tilde{p}}+t^f_i+t_{ijs}\le t^c_{j\tilde{p}}+M\left(1-x_{ij\tilde{p}s}\right)\ \forall i\in I,j\in I^-,s\in S \quad (42)$$

$$t^u_{\tilde{p}}=\sum_{i\in I^-}\sum_{j\in I^-}\sum_{s\in S}\left(t^c_{i\tilde{p}}R^u_i+x_{ij\tilde{p}s}b_i\right)\Big/t^u \quad (43)$$

$$t^c_{i\tilde{p}}+t^f_i+t_{i0s}\le T+M\left(1-x_{i0\tilde{p}s}\right)\ \forall i\in I^-,s\in S \quad (44)$$

$$\sum_{i\in I^-}\sum_{j\in I^-}\sum_{s\in S}\left(t^c_{i\tilde{p}}R^u+x_{ij\tilde{p}s}b_i\right)\le\sum_{v\in V}q_v r_{\tilde{p}v} \quad (45)$$

$$t^c_{i\tilde{p}}\le M\sum_{j\in I}\sum_{s\in S}x_{ij\tilde{p}s}\ \forall i\in I^- \quad (46)$$

$$t^c_{i\tilde{p}}\ge 0\ \forall i\in I^- \quad (47)$$

$$t^T_i\le t^c_{i\tilde{p}}\ \forall i\in I^- \quad (48)$$

$$t^T_i\ge t^c_{i\tilde{p}}-M(1-\sum_{j\in I}\sum_{s\in S}x_{ij\tilde{p}s})\ \forall i\in I^- \quad (49)$$

$$t^T_i\ge 0\ \forall i\in I^- \quad (50)$$

$$t^T_i\le M\sum_{j\in I}\sum_{s\in S}x_{ij\tilde{p}s}\,\forall i\in I^- \quad (51)$$

In the above formulas, formula (31) is the objective function, which is the test number of the single-ship scheduling plan in the FGSM-RMM. The constraints of the FGSM-SM are similar to those of the FGSM; the only difference is that k is replaced by $\tilde{p}$, which means that the core function of the FGSM-SM is to generate $\tilde{p}$. Since the FGSM-SM is equivalent to the path-planning problem proposed by Kobayashi and Kubo (2010), it can be efficiently solved by the method they provided.

6. Numerical experiment

We use public information on websites as a reference and use C++ to write calculation programs. All tests were run on a computer with an Intel Core i5-7200U processor, having 8 GB RAM. This section contains two parts of the experiment. The first part is a speed sensitivity analysis, which focuses on testing the impact of speed changes on the fleet scheduling plan. The second part is a carbon tax sensitivity analysis, which mainly examines the impact of carbon tax policy changes on the fleet scheduling plan.

6.1. Generation of experimental data

Due to the prosperity of the ship leasing market, a large amount of ship information is open and transparent. Therefore, we can directly query the FPSO information, crude oil production speed, and the capacity, speed, operating cost and rent of each shuttle tanker. Based on website data (i.e., http://fpso.com/and http://www.cosl.com.cn/col/col42951/index.html), we randomly generate information such as the location of each FPSO and the amount of oil available. We assume that a company has one land-based port and 10 FPSOs, and their specific distribution is shown in Fig. 3.

6.2. Speed sensitivity analysis

We assume that there are 5 types of tankers (labeled A~E). According to **assumption IV**, the number of tankers of various types is sufficient to meet the needs of the formation of a tanker fleet. Each tanker has 5 design speeds. The fixed cost per unit time, the design speeds of each type of tanker and the variable cost per unit time are

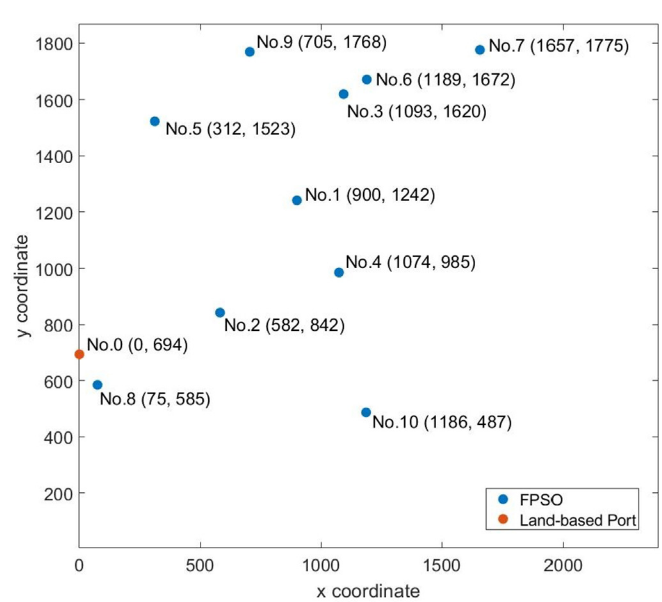

Fig. 3. The distribution of the land-based port and FPSOs.

Table 1
Basic operating parameters of shuttle tankers.

Tanker type	Capacity of the tanker (× 10^4 m^3)	Fixed cost per unit time (× 10^3 RMB/h)	Speed (knot)/Variable cost per unit time (× 10^3 RMB/h)				
			Design speed 1	Design speed 2	Design speed 3	Design speed 4	Design speed 5
A	6	2.4	7/2.8	10/4.1	13/5.6	16/6.9	19/7.9
B	12	2.7	6/3.0	9/4.6	12/6.3	14/7.6	17/9.3
C	17	3	5/3.5	8/5.4	11/7.0	13/8.6	16/10.5
D	18	3	5/3.5	8/5.4	11/7.0	13/8.6	16/10.5
E	22	3.3	5/3.9	8/6.0	11/7.7	13/9.4	15/12.0

Table 2
Comparison of optimization results between fixed speed and variable speed scenarios.

E1				E2			
Berthing order	Tanker type	Speed (knot)	Green operating cost (× 10^3 RMB)	Berthing order	Tanker type	Speed (knot)	Green operating cost (× 10^3 RMB)
0-8-0	A	13	2212	0-8-0	A	7–7	1842
0-2-10-0	D	11	25350	0-10-0	B	8–5	19876
0-1-7-0	E	11	43888	0-5-9-0	E	8-8-5	27015
0-9-5-0	E	11	29324	0-3-6-7-0	E	15-11-11-11	50469
0-4-3-6-0	E	11	37717	0-2-4-1-0	E	11-8-8-8	26190
Total green operating cost (× 10^3 RMB)			138491	Green operating cost (× 10^3 RMB)			125391
Running time (s)			59.76	Running time (s)			4.35

shown in Table 1.

We calculate the tanker fleet scheduling plan under two scenarios of fixed speed (E1) and variable speed (E2). In E1, the speed of each type of tanker is constant, taken from the “Design Speed 3” column in Table 1. In E2, each tanker will use the five different speeds shown in Table 1. The results of the two scenarios are shown in Table 2.

As shown in Table 2, E1 and E2 exhibit some differences in terms of fleet structure, tanker navigation paths and fleet green operating cost. In E1, to ensure the continuous production of the MOSS, it is necessary to use five tankers to form a fleet. The fleet includes three large oil tankers (E-type), one medium-sized tanker (D-type) and one small tanker (A-type). The A-type tanker is only responsible for the crude oil transportation service of the No. 8 FPSO. Under the setting that the tanker speed remains unchanged, the number of berthings with FPSOs by each tanker is small, and the flexibility of the shuttle tanker fleet is poor. Additionally, the economies of scale of the large oil tankers have not been fully utilized, and the efficiency of the tanker is lower in E1.

In E2, due to the adjustment space of the speed, the combination of large and small tankers avoids no-load operation to some extent. It is also worth noting that there are two complex routes (i.e., 0-3-6-7-0 and 0-2-4-1-0) in E2’s single-ship scheduling plan. These routes require two E-type shuttle tankers (220,000-ton class) to berth with three FPSOs, effectively exerting the economies of scale of large-scale tankers. On the one hand, the fleet operation plan in E2 utilizes the high-speed navigation mode to berth more FPSOs at one time; on the other hand, E2 reduces the carbon emissions of the fleet by reducing the speed of the tankers in some waterway links. Comparing the green operating cost of E1 and E2, the latter is reduced by approximately 9.5%. This reduction is mainly because when the tanker speeds are allowed to change, small tankers can increase their operational efficiency by increasing speed. Although the carbon emissions of these tankers may increase, leading to an increase in carbon tax expenditures, it can significantly reduce the use of large tankers, thereby reducing the total green operating cost of the fleet.

In summary, when the speed cannot be adjusted and the carbon tax only has a limited impact on the green operating cost, the best choice for the decision maker is to select smaller tankers. Decision makers can exploit the high operational efficiency of small tankers to offset the increased carbon tax on their use. In other words, speed adjustment is an effective way to form a fleet reasonably, improve the operating efficiency of different types of tankers, and reduce the green operating cost of the fleet.

Table 3
Green operating cost for different vessel speeds and variable cost.

Tanker type	Speed (knot)	Green operating cost (× 10^3 RMB/h)					
		S1	S2	S3	S4	S5	S6
A	7	3.5	4.6	5.2	6.9	9.1	11.4
	10	4.0	5.7	6.5	8.9	12.2	15.4
	13	4.6	6.9	8.0	11.4	15.8	20.3
	16	5.1	7.9	9.3	13.4	18.9	24.4
	19	5.6	8.8	10.3	15.0	21.3	27.7
B	5	3.9	5.1	5.7	7.5	9.9	12.2
	8	4.6	6.4	7.3	10.1	13.8	17.6
	11	5.2	7.7	9.0	12.8	17.8	22.9
	14	5.8	8.8	10.3	15.0	21.0	27.1
	17	6.4	10.1	12.0	17.6	25.0	32.4
C	5	4.4	5.8	6.5	8.6	11.4	14.2
	8	5.2	7.4	8.4	11.7	16.1	20.4
	10	5.8	8.6	10.0	14.2	19.8	25.4
	13	6.4	9.8	11.6	16.7	23.5	30.4
	16	7.2	11.4	13.5	19.8	28.2	36.6
D	5	4.4	5.8	6.5	8.6	11.4	14.2
	8	5.2	7.4	8.4	11.7	16.1	20.4
	11	5.8	8.6	10.0	14.2	19.8	25.4
	13	6.4	9.8	11.6	16.7	23.5	30.4
	16	7.2	11.4	13.5	19.8	28.2	36.6
E	5	4.8	6.4	7.2	9.5	12.5	15.6
	8	5.6	8.1	9.3	12.9	17.7	22.5
	11	6.4	9.5	11.0	15.6	21.8	27.9
	13	7.1	10.8	12.7	18.4	25.9	33.4
	15	8.1	12.9	15.3	22.5	32.0	41.6

6.3. Carbon tax sensitivity analysis

This section explores the impact of carbon taxes on decision makers’ decisions by changing variable cost c_{vs}^{V} and observing changes in the fleet scheduling plan. We set up 6 different scenarios

Table 4
Calculation results of S1~S6.

S1				S2			
Berthing order	Tanker type	Speed (knot)	Green operating cost ($\times 10^3$ RMB)	Berthing order	Tanker type	Speed (knot)	Green operating cost ($\times 10^3$ RMB)
0-3-6-7-0	E	15-11-11-11	27564	0-3-6-7-0	E	15-11-11-11	42174
0-1-4-0	C	8-8-5	12656	0-10-0	B	8–5	16350
0-8-0	A	7–7	1092	0-8-0	A	7–7	1504
0-5-9-0	D	13-11-8	15090	0-5-9-0	E	8-8-5	22829
0-2-10-0	D	11-8-5	13425	0-2-4-1-0	D	11-8-8-8	22172
Total green operating cost ($\times 10^3$ RMB)			69827	Total green operating cost ($\times 10^3$ RMB)			105029
Running time (s)			78.17	Running time (s)			10.99
S3				**S4**			
Berthing order	Tanker type	Speed (knot)	Green operating cost ($\times 10^3$ RMB)	Berthing order	Tanker type	Speed (knot)	Green operating cost ($\times 10^3$ RMB)
0-3-6-7-0	E	15-11-11-11	50469	0-3-6-7-0	E	15-11-11-11	71396
0-10-0	B	8–5	19876	0-10-0	B	8–5	26841
0-8-0	A	7–7	1842	0-8-0	A	7–7	2460
0-5-9-0	E	8-8-5	27015	0-5-9-0	E	8-8-5	37003
0-2-4-1-0	E	11-8-8-8	26190	0-2-4-1-0	E	11-8-8-8	36136
Total green operating cost ($\times 10^3$ RMB)			125391	Total green operating cost ($\times 10^3$ RMB)			173836
Running time (s)			3.99	Running time (s)			16.41
S5				**S6**			
Berthing order	Tanker type	Speed (knot)	Green operating cost ($\times 10^3$ RMB)	Berthing order	Tanker type	Speed (knot)	Green operating cost ($\times 10^3$ RMB)
0-3-6-7-0	E	15-11-11-11	100617	0-3-6-7-0	E	15-11-11-11	129838
0-4-1-0	C	8-5-8	41732	0-4-1-0	C	8-5-8	53771
0-8-0	A	7–7	3283	0-8-0	A	7–7	4239
0-5-9-0	E	8-8-5	51176	0-5-9-0	E	8-8-5	65349
0-2-10-0	E	8-5-8	45046	0-2-10-0	E	8-5-8	57308
Total green operating cost ($\times 10^3$ RMB)			241854	Total green operating cost ($\times 10^3$ RMB)			310505
Running time (s)			12.49	Running time (s)			11.67

(S1~S6). Each scenario is based on S3 and is obtained by changing the variable cost in proportions of 40%, 80%, 160%, 240%, and 320%, respectively. The green operating cost parameters are shown in Table 3.

The fleet scheduling plans and green operating cost of S1~S6 are shown in Table 4.

From the perspective of the fleet structure, the proportion of large tankers increases with increasing variable cost (carbon tax) from two E-type tankers in S1~S2 to three tankers in S4~S6. This phenomenon is consistent with our expectation. Unlike the previous sensitivity analysis, when the carbon tax rate continues to increase, the carbon tax that needs to be paid for the use of small tankers is significantly increased. However, the advantage of low carbon emissions per unit of cargo per unit distance of large tankers will gradually emerge. To reduce the carbon tax, a decision maker will increasingly use large tankers. However, the fleet always contains an A-type ship, which is due to the special location of the No. 8 FPSO. This location is closer to the port, and it is undoubtedly more economical to equip it with a small tanker. In summary, it is necessary to appropriately select large ships to berth several FPSOs at one time and give full play to the economies of scale of large-scale transportation vehicles.

From the perspective of tanker navigation routes and speed selection, with increasing carbon tax, there are three different tanker fleet scheduling plans, which are applied to S1, S2~S4 and S5~S6, respectively. As shown in the table, the navigation routes can be stabilized to some extent under different scenarios, and the tanker scheduling plan is further optimized only by speed and ship

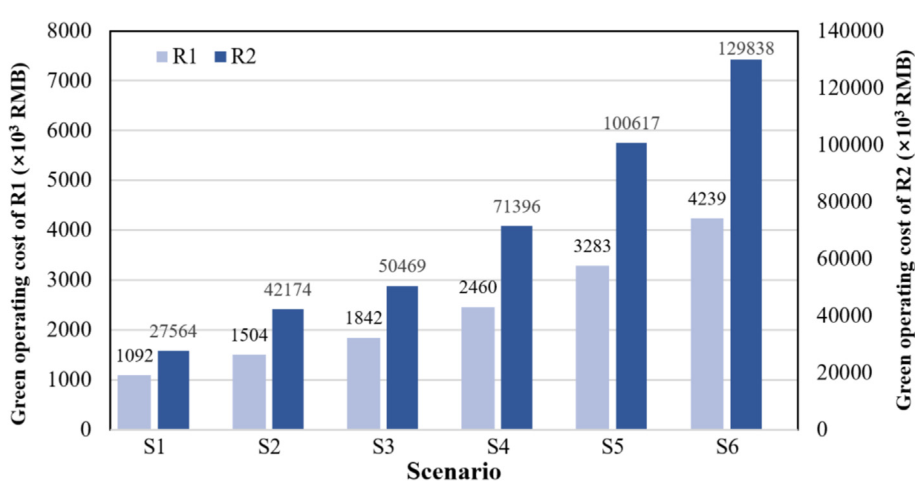

Fig. 4. The green operating cost of R1 and R2 in different scenarios.

type adjustment. For example, in S5~S6, the D-type tanker in S1 is changed to E-type, and the speeds of 13 knots and 11 knots are changed to 8 knots and 5 knots, respectively. The speed factor plays an important role in green scheduling. In addition, it is worth noting that in S1~S6, there are always two routes, "0-8-0" (R1) and "0-3-6-7-0" (R2), and their green operating cost in different scenarios are shown in Fig. 4.

Compared with S1, the green operating cost of the two routes in S6 increased by 288% and 371%, respectively. It can be seen that carbon-emission factors have a significant impact on fleet green scheduling. Additionally, the existence of the two routes indicates that there is a "critical task" in the MOSS, that is, the transportation task that must be completed to ensure continuous production. If a decision maker wishes to further optimize the green operating cost, he/she may need to further adjust the tanker type and speed.

To summarize, when the impact of the carbon tax on the transportation system is high enough, the best choice for decision makers is to use a large ship to berth several FPSOs at once to reduce the carbon tax. At this time, the cost reduction from the operational efficiency of the small tankers cannot cover the high carbon tax. Decision makers also need to address the bottleneck (i.e., "critical task") of the transportation system. When the existing tankers cannot be used to further reduce the green operating cost of the fleet through model change and speed adjustment, introducing new types of tankers and considering designing more speeds is a good choice.

7. Conclusion

(1) We propose a mathematical model for the green scheduling of shuttle tankers. The model realizes the green scheduling of the tanker fleet and reduces the crude oil company's green operating cost. Aiming at the characteristics of the model and relying on the CGA framework, we design an algorithm to solve the model accurately.

(2) By comparing the fixed speed and the variable speed, it is found that when the speed of the shuttle tankers can be adjusted, the green operating cost of the shuttle tanker fleet in the example is reduced by approximately 9.5%. Comparing the examples with different carbon taxes, we find that a higher carbon tax will guide the fleet's ship types toward the coordination and complementation of large and small tankers. Moreover, to further reduce green operating cost, decision makers should consider optimizing the bottleneck (i.e., "critical task") of the transportation system.

(3) The model we proposed in this paper also has some shortcomings. For example, we did not consider the amount of unloading operations of the shuttle tankers in each FPSO. When this value is determined, the green operating cost of the fleet can be further reduced. We also did not consider the queue of tankers at transport nodes (i.e., FPSOs and the land-based port). In fact, due to the limited number of berths, in practice, the ships are often congested at these transportation nodes. The above ideas can be used as an in-depth exploration of the future exploration direction of the research described in this paper.

Acknowledgments

The authors would like to express their gratitude to the support given by the National Natural Science Foundation of China [grant numbers 71402013, 71431001 and 71432007], the Humanity and Social Science Youth Foundation of the Ministry of Education of China [grant number 14YJC630010] and the China Postdoctoral Science Foundation [grant number 2014M551064].

References

Agarwal, R., Ergunx, Ö., 2008. Ship scheduling and network design for cargo routing in liner shipping. Transport. Sci. 42 (2), 175–196.
Alvarez, J.F., Tsilingiris, P., Engebrethsen, E.S., Kakalis, N.M., 2011. Robust fleet sizing and deployment for industrial and independent bulk ocean shipping companies. INFOR Inf. Syst. Oper. Res. 49 (2), 93–107.
Araújo, O.d.Q.F., de Carvalho Reis, A., de Medeiros, J.L., do Nascimento, J.F., Grava, W.M., Musse, A.P.S., 2017. Comparative analysis of separation technologies for processing carbon dioxide rich natural gas in ultra-deepwater oil fields. J. Clean. Prod. 155, 12–22.
Bektaş, T., Laporte, G., 2011. The pollution-routing problem. Transp. Res. Part B Methodol. 45 (8), 1232–1250.
Brouer, B.D., Alvarez, J.F., Plum, C.E., Pisinger, D., Sigurd, M.M., 2013. A base integer programming model and benchmark suite for liner-shipping network design. Transport. Sci. 48 (2), 281–312.
Chang, C.-C., Wang, C.-M., 2014. Evaluating the effects of speed reduce for shipping costs and CO2 emission. Transport. Res. Transport Environ. 31, 110–115.
Christiansen, M., Fagerholt, K., Nygreen, B., Ronen, D., 2013. Ship routing and scheduling in the new millennium. Eur. J. Oper. Res. 228 (3), 467–483.
Christiansen, M., Fagerholt, K., Ronen, D., 2004. Ship routing and scheduling: status and perspectives. Transport. Sci. 38 (1), 1–18.
Corbett, J.J., Wang, H., Winebrake, J.J., 2009. The effectiveness and costs of speed reductions on emissions from international shipping. Transport. Res. Transport Environ. 14 (8), 593–598.
Deng, H., Farah, P.D., Wang, A., 2015. China's role and contribution in the global governance of climate change: institutional adjustments for carbon tax introduction, collection and management in China. Social Science Electronic Publishing 8 (6), 1–35.
Deniz, C., Kilic, A., Cıvkaroglu, G., 2010. Estimation of shipping emissions in candarli gulf, Turkey. Environ. Monit. Assess. 171 (1–4), 219.
Fagerholt, K., Laporte, G., Norstad, I., 2010. Reducing fuel emissions by optimizing speed on shipping routes. J. Oper. Res. Soc. 61 (3), 523–529.
Ford Jr., L.R., Fulkerson, D.R., 1958. A suggested computation for maximal multicommodity network flows. Manag. Sci. 5 (1), 97–101.
Hoff, A., Andersson, H., Christiansen, M., Hasle, G., Kketangen, A., 2010. Review: industrial aspects and literature survey: fleet composition and routing. Comput. Oper. Res. 37 (12), 2041–2061.
Jian, L., Qin, S., Li, M., 2017. Production and transportation outsourcing decisions in the supply chain under single and multiple carbon policies. J. Clean. Prod. 141, 1109–1122.
Kobayashi, K., Kubo, M., 2010. Optimization of oil tanker schedules by decomposition, column generation, and time-space network techniques. Jpn. J. Ind. Appl. Math. 27 (1), 161–173.
Li, J., Wang, D., Zhang, J., 2018. Heterogeneous fixed fleet vehicle routing problem based on fuel and carbon emissions. J. Clean. Prod. 201, 896–908.
Niu, Y., Yang, Z., Chen, P., Xiao, J., 2018. Optimizing the green open vehicle routing problem with time windows by minimizing comprehensive routing cost. J. Clean. Prod. 171, 962–971.
Olmer, N., Comer, B., Roy, B., Mao, X., Rutherford, D., 2017. Greenhouse Gas Emissions from Global Shipping, 2013–2015. The International Council on Clean Transportation, pp. 1–38.
Oreskes, N., 2011. Metaphors of warfare and the lessons of history: time to revisit a carbon tax? Clim. Change 104 (2), 223–230.
Ronen, D., 1983. Cargo ships routing and scheduling: survey of models and problems. Eur. J. Oper. Res. 12 (2), 119–126.
Sepehri, A., Sarrafzadeh, M.-H., 2018. Effect of nitrifiers community on fouling mitigation and nitrification efficiency in a membrane bioreactor. Chemical Engineering and Processing-Process Intensification 128, 10–18.
Sun, D.-Q., Yi, B.-W., Xu, J.-H., Zhao, W.-Z., Zhang, G.-S., Lu, Y.-F., 2018. Assessment of CO2 emission reduction potentials in the Chinese oil and gas extraction industry: from a technical and cost-effective perspective. J. Clean. Prod. 201, 1101–1110.
Tirado, G., Hvattum, L.M., Fagerholt, K., Cordeau, J.-F., 2013. Heuristics for dynamic and stochastic routing in industrial shipping. Comput. Oper. Res. 40 (1), 253–263.
Xiao, Y., Konak, A., 2017. A genetic algorithm with exact dynamic programming for the green vehicle routing & scheduling problem. J. Clean. Prod. 167, 1450–1463.
Zhang, C., Nemhauser, G., Sokol, J., Cheon, M.-S., Keha, A., 2018. Flexible solutions to maritime inventory routing problems with delivery time windows. Comput. Oper. Res. 89, 153–162.
Zhang, Z.X., Baranzini, A., 2004. What do we know about carbon taxes? An inquiry into their impacts on competitiveness and distribution of income. Energy Policy 32 (4), 507–518.